# Elaboration of a Multispecies Model of Solid Tumor Growth with Tumor-Host Interactions

**A. Konstorum, S. A. Sprowl, A. D. Lander, M. L. Waterman and J. S. Lowengrub**

**Abstract** There has been increasing evidence of the critical effects of microenvironmental influence on tumor growth and metastasis. In this report, we extend a multispecies continuum model of solid tumor growth to include interaction of the tumor with its microenvironment. This new model, which incorporates reported interactions between tumor- and stroma-derived chemical signals, predicts a nonlinear response to host factors: increased growth and asymmetry of the tumor at low levels of stromal fibroblast-produced Hepatocyte Growth Factor / Scatter Factor (HGF/SF), and reduced growth at high levels.We test the model predictions using colon cancer initiating cell (CCIC) spheroids grown in media in varying concentrations of HGF. The experiments show qualitatively similar behavior to the model predictions. We plan to use the experimental studies to calibrate the mathematical model, and to use the mathematical model to make predictions regarding tumor behavior in order to guide future experimental studies.

A. Konstorum (✉)
Department of Mathematics, UC, Irvine, USA
e-mail: akonstor@uci.edu

S.A. Sprowl · M.L. Waterman
Department of Microbiology and Molecular Genetics, UC, Irvine, USA
e-mail: ssprowl@uci.edu

M.L. Waterman
e-mail: marian.waterman@uci.edu

A.D. Lander
Department of Developmental and Cell Biologym, UC, Irvine, USA
e-mail: adlander@uci.edu

J.S. Lowengrub
Department of Mathematics, Department of Biomedical Engineering Center for Complex Biological Systems, UC, Irvine, USA
e-mail: lowengrb@math.uci.edu

V. In et al. (eds.), *International Conference on Theory and Application in Nonlinear Dynamics (ICAND 2012)*, Understanding Complex Systems,
DOI: 10.1007/978-3-319-02925-2_26, 

## 1 Introduction

The importance of the microenvironment in tumor growth and metastasis has been established with a large body of research [1–6]. Nevertheless, the molecular interactions between tumor and stroma-resident cells, and the changes in both tissues that these interactions facilitate, are still under intense study, especially as it has become evident that pharmaceutical targeting of the tumor alone may not account for cancer promoting factors that are produced in the tumor microenvironment [7].

The purpose of this study is to extend a recently developed stem-cell based multispecies model of a solid tumor to include stromal interactions that are well corroborated by experimental data. Numerical analysis of the mathematical model allows us to examine, in silico, various scenarios of tumor-host interactions, and to compare our results against the experimental literature. Ultimately, we hope to use the model to make predictions about potential avenues for future research in malignancy, as well as pharmaceutical applications.

## 2 Background: A Mathematical Model of a Solid Tumor with Multiple Cell Types

A multispecies continuum model based on lineage dynamics of different tumor cell types has recently been developed by Youssefpour et al. [8]. As this model is extended here to incorporate tumor-host interactions, an overview of the model is necessary to understand the additions. Figure 1 summarizes the biological foundation of the model, while Fig. 2 summarizes the relevant equations.

## 3 Incorporating Host Effects

It has been shown in numerous studies that HGF production by cancer-associated fibroblasts in the stroma causes increased $\beta$-catenin localization in the nucleus of tumor cells near the tumor-host boundary, and additionally causes these cells to display properties of cancer stem cells such as increased migratory capacity and clonogenic potential [9, 10]. The effects of HGF can be attributed to binding of HGF to the c-Met receptor, which is expressed on tumor cells, and can result in a signaling cascade that ultimately leads to dissociation of $\beta$-catenin from its cytosolic partners and translocation into the nucleus where it can potentiate the canonical Wnt signal activity [11]. Based on these studies, we modify the equation for Wnt signaling, which represents the combined effects that promote Wnt signaling, such that concentration of HGF has a positive linear effect on Wnt signal production:

Elaboration of a multispecies model of solid tumor growth with tumor-host interactions.

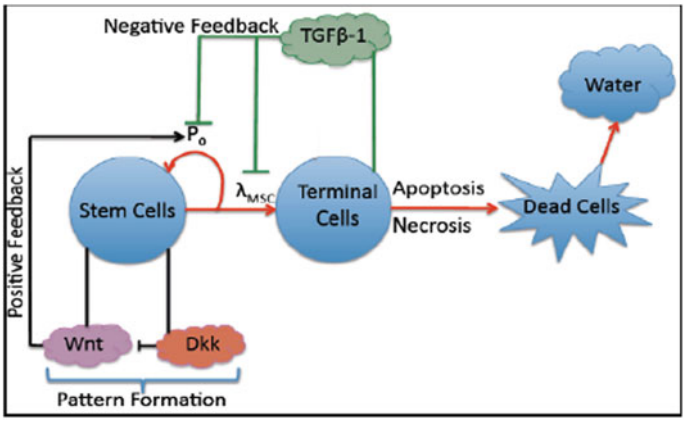


**Fig. 1** A multispecies model of tumor signaling: Tumor tissue is composed of three cell types: cancer stem cells (CSCs), terminally differentiated cells (TCs), and dead cells (DCs). Stem cells have a probability of self renewal $P_0$, differentiate into TCs with probability $1 - P_0$, and divide at a rate $\lambda_{MSC}$. $P_0$ is promoted by Wnt (and other autocrine) signals produced by the stem cells, which are in turn inhibited by Dkk (and other) proteins, also produced by CSCs. TCs secrete proteins from the TGF$\beta$ superfamily that lower $P_0$ and $\lambda_{MSC}$. CSCs and TCs can become DCs by apoptosis or necrosis. Adapted from [8]

$$\frac{\partial C_{Wnt}}{\partial t} = \nabla \cdot (D_{Wnt} \nabla C_{Wnt}) + f\,(C_{Wnt}, C_{Dkk}) \tag{1}$$

$$f\,(C_{Wnt}, C_{Dkk}) = \nu_{PWnt} \frac{\lambda_{HGF} C_{HGF} + C_{Wnt}^2}{C_{Dkk}} C_0 \phi_{CSC} - \nu_{DWnt} C_{Wnt} + \mu_0 C_0\,(\phi_T - \phi_{DC})\,, \tag{2}$$

where the HGF-induced production of Wnt signaling is modeled in the first term of the right-hand side of Eq. (2). Creating a model for HGF concentration is a more difficult matter, as there have been far fewer studies on the molecular basis for changes in HGF production by cancer-associated stromal cells. There have been many studies that have shown a direct effect of cancer cells on HGF production via their secretion of growth factors and cytokines such as TNF$\alpha$, bFGF, and PDGF that bind to the EGF receptor on stromal cells and cause upregulation of HGF production [2, 12]. Thus, we cannot currently specify whether the stem cells preferentially release these growth factors and if increased $\beta$-catenin localization (via HGF signaling) results in an increased release of these factors from neighboring tumor cells, which would indicate a positive feedback mechanism. With the data available, we model a positive effect of growth factors from viable tumor tissue on HGF production in the stroma. Additionally, there is substantial evidence that TGFb is a negative regulator of HGF production in stromal cells, and thus we include its inhibitory effect in the model (2):

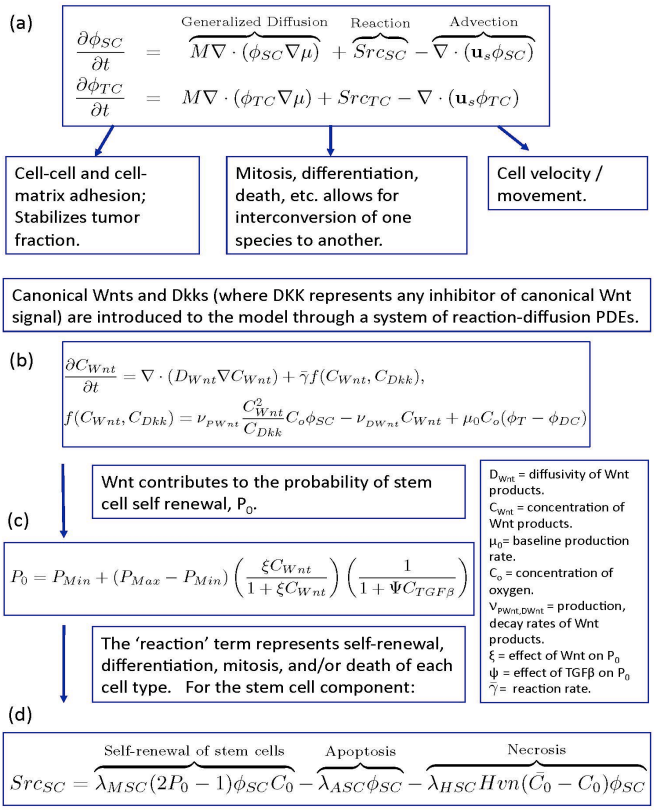


**Fig. 2** Modeling the multispecies tumor: A brief outline of the model is given here. For a more detailed description, see [8]. The functions $\phi_{SC}$, $\phi_{TC}$ (shown) and $\phi_{DC}$, $\phi_W$, $\phi_H$ (not shown) represent the local fractions of CSC, TC, and DC populations in lineage and the water and host cells, respectively. The sum of the volume fractions equals 1. **a** For each cell type, the conservation equation is posed, where $J = -M\phi\nabla\mu$ is a generalized flux (or cellular diffusion), $Src$ is the mass-exchange term, and us is the mass-averaged velocity of the solid components, assumed to satisfy Darcys law and is given by $\nabla\cdot u_s = Src_{SC} + Src_{TC} + Src_{DC}$. Cells are assumed to move with the mass-averaged velocity. For$J = -M\phi\nabla\mu$, $M$ is the mobility and $\mu$ is the chemical potential, which is proportional to the variational derivative of the adhesion energy. The flux is derived from an adhesion energy that accounts for interactions among the cells. **b** We account for a self-renewal promoter, such as Wnt, which increases the self-renewal fraction of CSCs, and an inhibitor of the self-renewal promoter, such as Dkk, using a generalized Geierer-Meinhardt-Turing system of reaction-diffusion equations. Both are only produced by CSCs, and Wnt diffusion range is assumed to be shorter than that of Dkk. **c** CSC self-renewal fraction, $P_0$ is positively regulated by Wnt and negatively regulated by TGF$\beta$ with $\xi$ and $\Psi$ the feedback response of the CSCs to the respective proteins. **d** Source term for CSCs. Proportion of CSCs are increased by mitosis rate of CSCs, $\lambda_{MSC}$, that are self-renewing, and is dependent on $C_0$, the local concentration of oxygen and nutrients. $Hvn(x)$ denotes the Heaviside function, which is equal to 1 when $x > 0$ and 0 otherwise. $\bar{C}_0$ denotes the minimum level of oxygen and nutrients required for cell viability. $Src_{TC}$ and $Src_{DC}$ are modeled analogously

$$\frac{\partial C_{HGF}}{\partial t} = \nu_{PHGF} \frac{C_{GF}}{\xi + \lambda_{TGF\beta} C_{TGF\beta}} C_0 \phi_H + \overbrace{\eta_0 C_0 \phi_0}^{\text{HGF background production rate}} - \overbrace{\nu_{DHGF} C_{CHGF}}^{\text{HGF decay/ binding rate}} + \nabla \cdot (D_{HGF} \nabla C_{HGF}), \quad (3)$$

where the inhibition by TGFb and promotion by tumor-produced growth factors is modeled in the first term of the right-hand side of Eq. (3).

As discussed above, HGF-promoting growth factors are released by tumor cells, but it is not known whether the production of these growth factors is different in stem and differentiated cells. Thus, we allow for the production rate of growth factors to be different for each of the cell types:

$$\frac{\partial C_{HGF}}{\partial t} = \nabla \cdot (D_{GF} \nabla C_{GF}) + \overbrace{C_0 \left(\nu_{GFS} \phi_{CSC} + \nu_{GFT} \phi_{TF}\right)}^{\text{Growth Factor production rate}} - \overbrace{\nu_{DFG} C_{GF}}^{\text{Growth Factor decay / binding rate}} \quad (4)$$

We refer the reader to Table 1 for description of the variable and parameter symbols.

## 4 Numerical and Experimental Methods

For the nondimensionalization and numerical implementation, we followed a previously published numerical method, which we briefly describe here [8]. An adaptive finite difference-nonlinear multi grid method [13, 14] was used to solve the governing equations efficiently. For reasons described in [8, 13], we solved for $\phi_T = \phi_{CSC} + \phi_{TC} + \phi_{DC}$. To remove a high-order time step constraint incurred by an explicit method, we used an implicit 2nd order accurate time discretization of Crank-Nicholson type, and spatial derivatives were discretized using 2nd order accurate central difference approximations. In regions of large gradients, block structured Cartesian refinement was used to provide enhanced local resolution.

In the experiments, colon cancer initiating cells (CCICs) were cultured as spheroids in ultra-low attachment flasks (Corning) using DMEM/F12 50:50 supplemented with N2, B12, EGF, bFGF, heparin, sodium pyruvate, and penicillin/ streptomycin [15]. Unlike typical cell lines, CCICs are multipotent and capable of regenerating heterogeneous tumors with characteristics analogous to those found in primary tumors, from which they are derived [15, 16]. CCICs were trypsinized using a no-serum trypsin inhibitor. Single cells were counted and plated in 96 well ultra-low attachment plates (Corning) using the previously mentioned media with or without HGF at various concentrations. CCICs were imaged at 10x resolution once each day. Cell clusters were observed for sphere morphology and size. Sphere size was determined by outlining the major sphere boundary (excluding scattered or shed cells) using ImageJ. Average volume increase over day 3 from three experimental trials was calculated in order to allow the spheroids 72 hours to adapt to new media.

| Variable or parameter | Description | Value | Reference and / or rationale (if not in text) |
|---|---|---|---|
| $\phi_H$ | stromal fraction (=1-$\phi_T$ ) | | |
| $C_{HGF}$ | concentration of HGF | | |
| $C_{GF}$ | concentration of HGF- promoting factors | | |
| $D_{GF}$ | diffusion coefficient for GF | 1.0 | [17, 18] |
| $D_{HGF}$ | diffusion coefficient for HGF | 0.1 | Set to a value lower than for GF due to higher molecular weight of HGF and necessity for HGF to be processed by molecules in ECM before it can bind to c-MET [19]. |
| $\lambda_{HGF}$ | strength of Wnt induction by HGF | 1.0 | Optimal reference data not available, plan to calibratein future experiments. |
| $\lambda_{TGF\beta}$ | inhibitory effect of TGFb on HGF production | 1.0 | [20] |
| $\eta_0$ | background HGF production rate by non-cancer associated stromal cells | 0.0001 | Set to a value significantly lower than GF-induced production levels [21]. |
| $\nu_{PHGF,DHGF}$ | induction, decay rates of HGF | 0.1, 1.0 | [12, 19] |
| $\nu_{GFS,GFT}$ | production rates of GF modeled by stem and differentiated cells, respectively | 0.1, 0.1; 10,10 | Varies widely by cell type [22]. Here, at low and high levels. Levels set to be equal in both conditions since differential production rate information not available. |

## 5 Results

Numerical results from incorporation of low HGF signal, created by a lower production rate of growth factors ($\nu_{GFS,GFT} = 0.1$) resulted in increased tumor asymmetry, instability, and volume when compared to the no host simulation (Fig. 3a, b; No host and Host: low HGF categories). By increasing growth factor production rate ($\nu_{GFS,GFT} = 10$), maximal HGF levels at the tumor-host boundary were increased approximately 100-fold (Fig. 3c), and resulted in a nonlinear growth response to HGF, namely at higher HGF levels, the tumor had greater symmetry and lower growth rate than at low HGF (Fig. 3, Host: high HGF category).

Experiments were performed to corroborate results of the model with primary colon cancer initiating cell (CCIC) spheroids grown in increasing concentration of HGF. Spheroids are a relevant model for tumor growth since they can be used to examine 3-dimensional properties of growing tissues, which more closely resemble in vivo tumors than 2-dimensional culture models (23). The experimental results show increasing spheroid growth rate with increasing concentration of HGF up to 100 ng/ml, but decreased growth and asymmetry at 250 ng/ml as compared to lower levels of HGF (Fig. 4), which is qualitatively consistent with the model predictions.

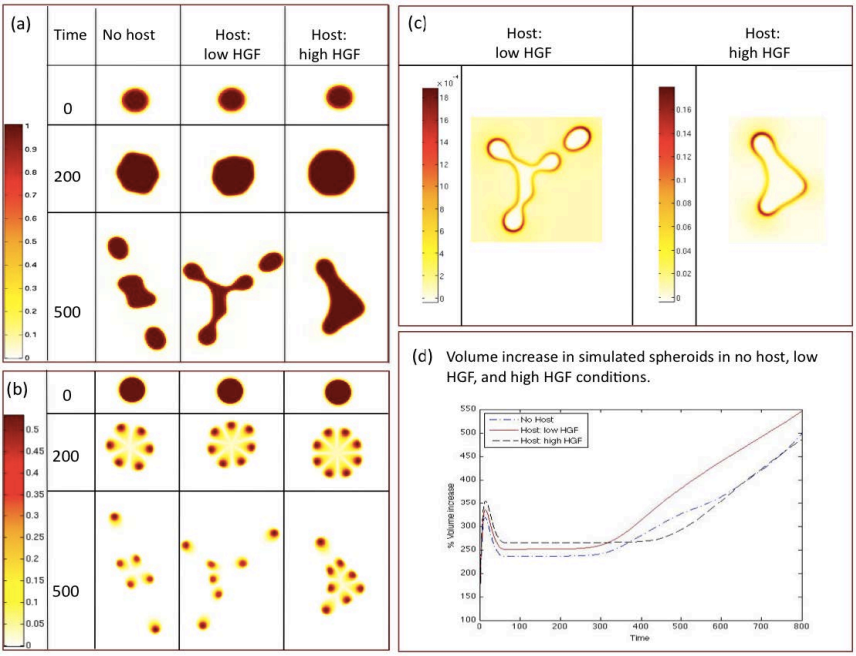


**Fig. 3** Simulation results of tumor-host model: Visualization of numerical results of the mathematical formulation for incorporation of host factors (HGF) at low and high levels into a multispecies model for **a** total tumor, **b** stem cell fraction, and **c** HGF concentration (note difference in scale). **d** Tumor volume is increased in low HGF environment, but decreases in increased concentration of HGF

## 6 Discussion

We have created a mathematical model for tumor-host interactions by incorporating chemical interactions between host and tumor tissues into a multispecies continuum model of tumor growth. Our theoretical results at low HGF indicate a good match to the literature, namely that inclusion of host interactions increased tumor growth rate and dispersion, as well as stem cell concentration at the tumor-host boundary, over the no host model. The non-monotonic response is due to decrease in heterogeneity of cell species at the tumor-host boundary resulting from an increased concentration of stem cells in that region. This leads to more uniform growth, ie. less branching over time than what is found in the low HGF model. Indeed, it has recently been shown that at high concentrations of HGF, myogenic stem cells become quiescent, while at lower concentrations, they proliferate and differentiate [23].

While our model matches experimental observations qualitatively, our ultimate goal is to create an experimentallycalibrated mathematical model that can be used, in conjunction with experimental verification, to make testable predictions about tumor behavior in various conditions, including presence of stroma and subsequent therapy. To this end, we have begun an experimental collaboration using tumor spheroids

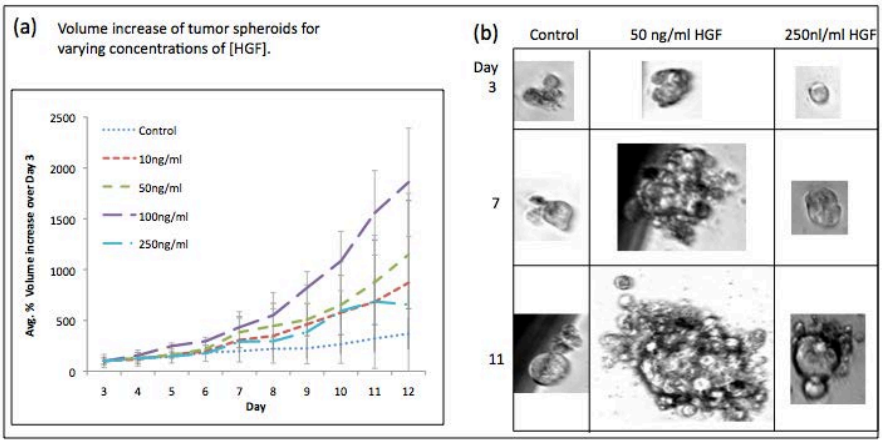


**Fig. 4** Tumor spheroid culture with increasing [HGF]: CCIC tumor spheroids were grown in media with increasing concentration of HGF. **a** Average volume increase (from day 3) of three experimental trials / day. **b** Sample images from spheroids grown in control (left column), +50 ng/ml HGF media (*center column*), and +250 ng/ml HGF media (*right column*)

developed with the CCIC cell line [15, 16]. While the current experiments did not include feedback from tumor onto stroma, but only addition of HGF at increasing concentrations in the media, there is still strong resemblance of the model to the experiment as the interactions in the model serve to increase the effective HGF at the tumor-host boundary, which is mimicked by higher concentrations in the experimental media. The experimental observations show both an increase in tumor area and increased asymmetry and dispersiveness of the tumor at lower concentrations of HGF, and a slower growth rate and higher tumor symmetry at high levels of HGF (Fig. 4), indicating similarity of outcomes between the model and experiment.

Work is currently in progress to calibrate our numerical model to the experimental system by matching the growth parameters and timescale of the experimental system, removing feedback to stroma, and incorporating the nonlinear effect of HGF at higher concentrations on tumor growth. The framework of the calibrated model remains the same as to what is presented in this paper.

In parallel, the experimental system is also being developed to include a co-culture with stroma and staining for stem and other cell types in order to better match our current model, which is more closely aligned with the in vivo dynamics of HGF action on tumor growth. Furthermore, we plan to incorporate, into both the numerical and experimental system, the following: quantification and modeling of cell spread, tumor angiogenesis, and macrophage involvement in tumor growth. Our long-term goal is to build a predictive model that can be efficiently used to better understand tumor physiology and response to treatment.

**Acknowledgments** The authors would like to thank the National Institutes of Health and the National Cancer Institute for funding through grants 1RC2CA148493-01 and P30CA062203 for

the Chao Comprehensive Cancer Center at UC Irvine. In addition, we acknowledge partial support from NIH grant P50GM76516 for a Center of Excellence in Systems Biology at UC Irvine. Further, AK gratefully acknowledges support from National Institutes for BioImaging and Bioengineering, JSL for support from the National Science Foundation, Division of Mathematical Sciences, and MLW for support from NIH grants CA096878 and CA108697.

## References

1. T. Borovski, E. De Sousa, F. Melo, L. Vermeulen, J.P. Medema, Feb 2011 Cancer Res. **71**(3), 634–639 (2011)
2. K. Matsumoto, T. Nakamura, Int. J. Cancer **119**(3), 477–483 (2006)
3. D. Hanahan, R.A. Weinberg, Cell **144**(5), 646–674 (2011)
4. A. Orimo, R.A. Weinberg, Cell Cycle **5**(15), 1597601 (2006)
5. K. Pietras, A. Ostman, Exp. Cell Res. **316**(8), 132431 (2011)
6. D. Hanahan, L.M. Coussens, Cancer Cell **21**(3), 30922 (2012)
7. P.A. Kenny, G.Y. Lee, M.J. Bissell, Front Biosci **12**(3468), 74 (2007)
8. H. Youssefpour, X. Li, A.D. Lander, J.S. Lowengrub, J. Theor. Biol. **304**(39), 59 (Jul 2012)
9. L. Vermeulen, E. De Sousa, F. Melo, M. van derHeijden, K. Cameron, J.H. deJong, T. Borovski, J.B. Tuynman, M. Todaro, C. Merz, H. Rodermond, M.R. Sprick, K. Kemper, D.J. Richel, G. Stassi, J.P. Medema, Nat. Cell Biol. **12**(5), 468–476 (2010)
10. A. Kaminski, J.C. Hahne, E.-M. Haddouti, A. Florin, A. Wellmann, N. Wernert, Int. J .Mol. Med. **18**(5), 941–950 (2006)
11. G. Banumathy, P. Cairns, Cancer Biol. Ther. **10**(7), 658–664 (2010)
12. A. De Luca, M. Gallo, D. Aldinucci, D. Ribatti, L.D. Lamura, A. Alessio, R. De Filippi, A. Pinto, N. Normanno, J. Cell Physiol. **226**(8), 21318 (2011)
13. S.M. Wise, J.S. Lowengrub, H.B. Frieboes, V. Cristini, J. Theor. Biol. **253**(3), 52443 (2008)
14. S.M. Wise, J. Sci. Comput. **44**(1), 38–68 (2010)
15. S.S. Sikandar, K.T. Pate, S. Anderson, D. Dizon, R.A. Edwards, M.L. Waterman, S.M. Lipkin, Cancer Res. **70**(4), 146978 (2010)
16. L. Ricci-Vitiani, D.G. Lombardi, E. Pilozzi, M. Biffoni, M. Todaro, C. Peschle, R. De Maria, Nature **445**(7123), 1115 (2007)
17. N. Quarto, F.P. Finger, D.B. Rifkin, J. Cell Physiol. **147**(2), 3118 (1991)
18. D.F. Bowen-Pope, R. Ross, Clin. Endocrinol. Metab. **13**(1), 191–205 (1984)
19. O. Holmes, S. Pillozzi, J.A. Deakin, F. Carafoli, L. Kemp, P.J.G. Butler, M. Lyon, E. Gherardi, J. Mol. Biol. **367**(2), 395–408 (2007)
20. K. Matsumoto, H. Tajima, H. Okazaki, T. Nakamura, J. Biol. Chem. **267**(35), 2491720 (1992)
21. S.-W. Tyan, W.-H. Kuo, C.-K. Huang, C.-C. Pan, J.-Y. Shew, K.-J. Chang, E.Y.-H.P. Lee, W.-H. Lee, PLoS One **6**(1), e15313 (2011)
22. T. Nakamura, K. Matsumoto, A. Kiritoshi, Y. Tano, T. Nakamura, Cancer Res. **57**(15), 330513 (1997)
23. M. Yamada, R. Tatsumi, K. Yamanouchi, T. Hosoyama, S.-i. Shiratsuchi, A. Sato, W. Mizunoya, Y. Ikeuchi, M. Furuse, R.E. Allen, Am. J. Physiol. Cell Physiol. **298**(3), C46576 (2010)